THE ASTROPHYSICAL JOURNAL, 460:601–611, 1996 April 1

SPECTRAL AND SPATIAL ANALYSIS OF THE INTRAGROUP MEDIUM IN THE NGC 2300 GROUP

DAVID S. DAVIS
Department of Physics and Astronomy The University of Alabama, 206 Gallalee Hall, Tuscaloosa, AL 35487
JOHN S. MULCHAEY
The Observatories of the Carnegie Institution of Washington, 813 Santa Barbara Street, Pasadena, CA 91101-1292
RICHARD F. MUSHOTZKY
Laboratory for High Energy Astrophysics NASA/Goddard Space Flight Center, Code 666, Greenbelt, MD 20771
AND
DAVID BURSTEIN
Department of Physics and Astronomy, Arizona State University, Tempe, AZ 85287-1504
Received 1995 June 1; accepted 1995 October 18

ABSTRACT

We report the results of spectral and spatial analysis of three overlapping *ROSAT* PSPC observations of the NGC 2300 group. Spatial analysis of the co-added fields reveals that the diffuse X-ray gas can be traced to at least 25′ (0.33 Mpc, $H_0 = 50$ km s^{-1} Mpc^{-1}). The surface brightness of the gas is well fitted with an isothermal King model with a core radius of $4\farcm28^{+1.27}_{-0.93}$ ($56.5^{+16.8}_{-12.3}$ kpc) and a β of $0.410^{+0.027}_{-0.021}$. The temperature of the gas, as determined from fitting a Raymond-Smith plasma model to the spectral data, is $0.97^{+0.11}_{-0.08}$ keV. The additional exposure time obtained allows three different annuli to be fitted. Fitting these different regions constrains any temperature gradient to be less than $\sim$0.2 keV. The abundance determined from the X-ray spectrum is also low—less than 0.11 solar. The mass of gas within 0.33 Mpc is $1.25 \times 10^{12}\ M_\odot$, and if the gas is in hydrostatic equilibrium with the potential the total mass within this radius is $1.47 \times 10^{13}\ M_\odot$. Comparing the mass of the galaxies plus the mass of hot gas to the total mass of the system yields an observed baryonic fraction of 10%–16%. This value is higher than our original analysis, where the form of the gas density profile was fixed at an assumed value. We also discuss the abundance of the diffuse gas and how the evolution of the elliptical galaxy is expected to affect the gas.

Subject headings: diffuse radiation — galaxies: clusters: individual (NGC 2300) — intergalactic medium — X-rays: galaxies

1. INTRODUCTION

The NGC 2300 group was the first poor group of galaxies to have hot diffuse gas detected in it (Mulchaey et al. 1993). The presence of hot gas in poor groups is significant for several reasons. First, it provides strong evidence that these groups are bound. Second, since the hot gas should trace the potential well of the groups such data will allow an accurate mass to be determined from X-ray imaging spectroscopy. Third, compared to galaxy clusters, groups of galaxies are relatively simple systems, and testing different scenarios for heating and enrichment of the gas is possible. This gas is also an important indicator of the dynamical state of the group. Finally, in hierarchical clustering theory groups of galaxies form from relatively small fluctuations in the initial background and should be a "fairer" sample of the universe than clusters of galaxies. Consequently, the measurement of the spatial distribution of hot gas in poor groups provides important cosmological constraints.

Since the initial analysis of the NGC 2300 group many more groups have had X-ray emission detected (Mulchaey et al. 1996; Davis et al. 1995; Pildis, Bregman, & Evrard 1995; David, Forman, & Jones 1995; Saracco & Ciliegi 1995; Böhringer 1994; David et. al. 1994; Thiering & Dahlem 1996; Sulentic, Pietsch, & Arp 1994; Ponman & Bertram 1993). These new data confirm the basic result reported by Mulchaey et al. (1993) that poor groups of galaxies are massive enough to retain hot X-ray emitting gas and that most of the mass is in the form of dark matter. These groups all have cool temperatures, $kT < 1.4$ keV, but the fitted abundances vary widely, from a low of $\sim$0.02 to a high of $\sim$0.8 solar.

The diffuse gas in poor groups is difficult to study because of its low surface brightness and low luminosity. Obtaining sufficient counts requires deep exposures, and separating the group signal from the background is difficult. Only a few of the groups detected with the *ROSAT* PSPC have adequate counts for the global properties of the group to be well determined. Fewer still have enough counts to measure the temperature and abundance at various radii. These considerations make detailed studies of many groups challenging. As such, a detailed study of one group can shed additional light on the properties of hot gas in poor galaxy groups. The object of this detailed study is to determine the physical parameters of the NGC 2300 group more accurately. Therefore, we obtained two additional deep PSPC exposures of this group. These data allow us to more accurately determine the extent of the group gas, measure any temperature or abundance gradients, and thus better constrain the physical parameters of the gas and the group.

We present the spatial and spectral analysis of all three *ROSAT* observations of the NGC 2300 group, including the initial PSPC observation presented by Mulchaey et al. (1993). Section 2 presents the observations and how they were processed. The spatial analysis of the group is presented in § 3. Results of the integrated group spectrum along with results for the spatially resolved spectra of the group

are presented in § 4, while in § 5 the total mass of the group is determined. The implications of the low-abundance diffuse X-ray gas is discussed in § 6, and our conclusions are presented in § 7.

2. OBSERVATIONS

The initial detection of gas in the NGC 2300 group was from the analysis of a single *ROSAT* PSPC pointing, which centered the group in the PSPC FOV (field of view) (Mulchaey et al. 1993). The low surface brightness of the diffuse emission makes the detection of this gas difficult against the relatively bright X-ray emission of our own Galaxy and the extragalactic X-ray background. To constrain the physical properties of the group gas more accurately, we obtained two additional PSPC observations of this group (Table 1).

These additional pointings were offset from the center of the diffuse gas so that any detector artifacts would be identifiable in the data sets. The X-ray data analyzed here consists of three separate pointings, one centered on the group, one offset to the east by $\sim 7'$ and one offset to the west by $\sim 14'$. The galaxies NGC 2300 and NGC 2276 are detected in all three pointings and are within the 20′ central ring of the PSPC support structure. We assume that the distance to this group is 45.7 Mpc, which comes from the local group radial velocity of the NGC 2300 group and an assumed value of $H_0 = 50$ km s^{-1} Mpc^{-1} for the Hubble constant.

The pointing positions and exposure times for all three data sets used in this analysis of the NGC 2300 group are presented in Table 1 along with the sequence number of the observation. The exposure times given are the final times included in the data sets after the data were "cleaned," as described below. The final usable exposure time was 22,720 seconds for all three sequences combined; almost a factor of 4 greater than the original 6035 s observation presented in Mulchaey et al. (1993). The increased number of photons allows us to determine the surface brightness profile of the diffuse gas without *assuming* a value of β, the asymptotic slope of the gas density profile, as was necessary in the original analysis. The larger number of photons also allows us to divide the group into several annuli and investigate the radial dependence of the temperature and abundance.

The PSPC is sensitive to a variety of effects, such as the long-term enhancements (LTEs), scattered solar X-rays, particle events, and variations in the local X-ray background. These make the analysis of extended sources much more difficult than for point sources (Snowden et al. 1994). The procedures used to remove these effects from the PSPC data follow the procedures discussed in Davis et al. (1995), so will only be outlined below.

To eliminate X-rays from local sources, such as scattered solar X-rays and charged particle events detected as X-rays, we used the XSELECT software to interactively display the counting rate for the entire PSPC and examine this for times when the counting rate increased. This increased counting rate is usually caused by solar X-rays being scattered into the optical path of the telescope, either from the X-ray emission from the quiet Sun or from a solar flare. XSELECT was then used to exclude these times from the final data set. Data were also excluded from the final data set if the master veto rate exceeded 170 counts s^{-1}.

Point sources were also removed from the final image and spectrum of the diffuse gas by excluding a circular region around each source. For point sources within a radius of 20′ from the PSPC center, a radius of 3′ was used to exclude point source photons. We found that an exclusion radius of 3′ was also sufficient for NGC 2300 and NGC 2276, which are slightly extended. For sources at larger off-axis angles larger circles were used to account for the variation of the point spread function of the PSPC. All the radii were picked to remove at least 90% of the point source flux from the image or spectrum of the diffuse gas.

The PSPC has a strong low-energy response that makes it ideal for studying Galactic diffuse emission but that can interfere with study of extragalactic extended objects. At high Galactic latitudes we find that the Galactic emission is fairly uniform over the PSPC field of view ($\sim 2°$) and that using the background from the same PSPC observation provides an excellent estimate of the Galactic contribution. To reduce the uncertainty of the background contribution from the local soft X-ray background further we restrict our analysis to the energy range between 0.4 and 2.0 keV.

The background region used for both the spectral and spatial analysis of the diffuse gas is taken from an annulus with inner radius 40′ and an outer radius of 50′ after excluding all known point sources in that annulus. The images presented cover an energy range of 0.5–2.0 keV with the limits being set by the definition of the energy bands used to flat-field the data (Snowden et al. 1994). The energy range for fitting the spectra is from 0.4–2.0 keV, which has been chosen to reduce the effects of the Galactic background and LTEs on the source spectrum. Restricting the spectral fits to the same energy range as the imaging data (0.5–2.0 keV) only increases the spectral errors slightly and does not significantly change the results.

TABLE 1

ROSAT PSPC FIELDS

Sequence Number	R.A. (J2000)	Decl. (J2000)	Exposure (s)	Observation Date
800161.....	$7^h26^m53^s$	+85°45′00″	5134	1992 Apr 25–27
800512.....	$7^h21^m12^s$	+85°42′00″	9034	1993 Aug 22–23
800513.....	$7^h38^m48^s$	+85°42′00″	8427	1993 Aug 23

3. SPATIAL RESULTS

A contour plot of the combined PSPC data is shown in Figure 1 with the X-ray contours overlaying an optical image of the group. The X-ray data have been corrected for vignetting and for the nonuniform exposure over the FOV using the exposure maps as specified in Snowden et al. (1994). After each PSPC image was corrected, the fields were coaligned and co-added. To produce a map of the diffuse emission the point sources in the field were replaced with the average value from around the point source, as described in § 2, and in Davis et al. (1995).

Figure 2 shows the emission that remains after the point sources are removed and the data are smoothed with a Gaussian with $\sigma = 1.5$. The centroid of the diffuse emission is at $7^h30^m17^s.5$, +85°43′41″.3 (J2000), and we use this as the group center for extraction of the spatial and spectral data. The peak is 2.5 to the northwest of NGC 2300 and in the direction of NGC 2276, so the peak of the diffuse gas lies between the two principal galaxies of the group. The X-ray contours appear fairly symmetric in the central regions of the group but the X-ray contours may be slightly compressed in the direction of NGC 2276.

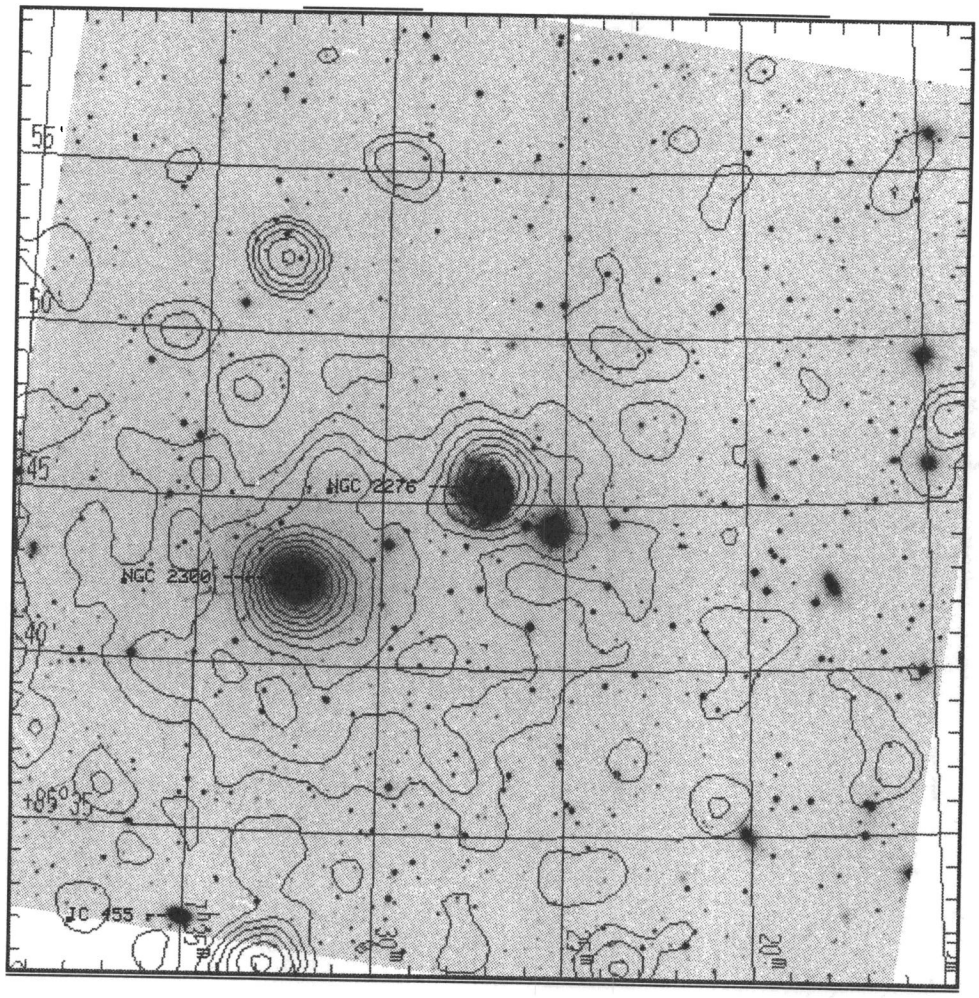

FIG. 1.—Combined PSPC data for the NGC 2300 group, smoothed by a Gaussian with $\sigma = 30''$ and overlaying an optical image from the digitized sky survey. The X-ray contours are (0.63, 0.90, 1.28, 1.82, 2.58, 3.66, 5.20, 7.38, 10.48, 14.88, 21.13) $\times 10^{-4}$ counts s^{-1} arcmin^{-2}.

The surface brightness profile of the group gas is extracted from the combined data set. The background for the spatial analysis is determined from the surface brightness profile of the diffuse gas *without* background subtraction. The profile is fitted with an isothermal β model (Cavaliere & Fusco-Femiano 1976) along with a constant to represent a uniform background in the field. This model fits the background region very well with a $\chi^2_\nu = 1.25$. The background derived from this fit is $2.39^{+0.36}_{-0.49} \times 10^{-4}$ counts s^{-1} arcmin^{-1}. This is in excellent agreement with the background value of $2.55 \pm 0.34 \times 10^{-4}$ counts s^{-1} arcmin^{-1} determined from the RASS (*ROSAT* All Sky Survey; R. Eggar 1994, private communication). Our background is less than the 3.21×10^{-4} counts s^{-1} arcmin^{-1} quoted by Pildis et al. (1995) using the original data and most likely accounts for the different results reported by Pildis et al. and our results. Errors listed throughout this work are the 90% confidence errors. The extracted profile for the data and the background is shown in Figure 3*a*. The background determined above is subtracted from the profile data, and the surface brightness profile for the group gas is shown in Figure 3*b* along with the fit to the data.

We fitted the group profile to the form

$$S(r) = S_0(1 + r^2/R^2_{\rm core})^{-3\beta+0.5}, \quad (1)$$

where S_0 is the central surface brightness, $R_{\rm core}$ is the core radius of the distribution, and β measures the asymptotic slope of the profile. This model fits the data well, $\chi^2_\nu = 1.10$ for 39 degrees of freedom, with a core radius of $4'.28^{+1.27}_{-0.93}$ ($56.5^{+16.8}_{-12.3}$ kpc) and a β of $0.410^{+0.027}_{-0.021}$. The emission from the peak of the group is $9.87^{+0.18}_{-0.16} \times 10^{-4}$ counts s^{-1} arcmin^{-1}.

Note that the peak of the group emission is only 4 times that of the background, so an accurate determination of the background is *critical* in determining the parameters of the group gas. To illustrate this point we have also analyzed profiles of the diffuse gas using the 90% upper and lower limits on the background contribution as the subtracted background. The King model fits the profile with the maximum background removal with a larger core radius (8'.05) and a steeper slope ($\beta = 0.60$). Using the minimum background decreases the core radius to 2'.57 and β to 0.33. Clearly, the accurate determination of the background is critical for determining the fitted parameters for groups.

4. SPECTRAL RESULTS

The spectrum of the diffuse gas was extracted using a circular region centered at the position of the peak emission given above and excluding flux from all known point sources. The total number of counts from the diffuse gas is ~6400 within a radius of 25'. Since the group is positioned in a different place in the detector for each observation, the vignetting corrections are also different for each spectrum. Thus, we cannot co-add the individual spectra and fit the

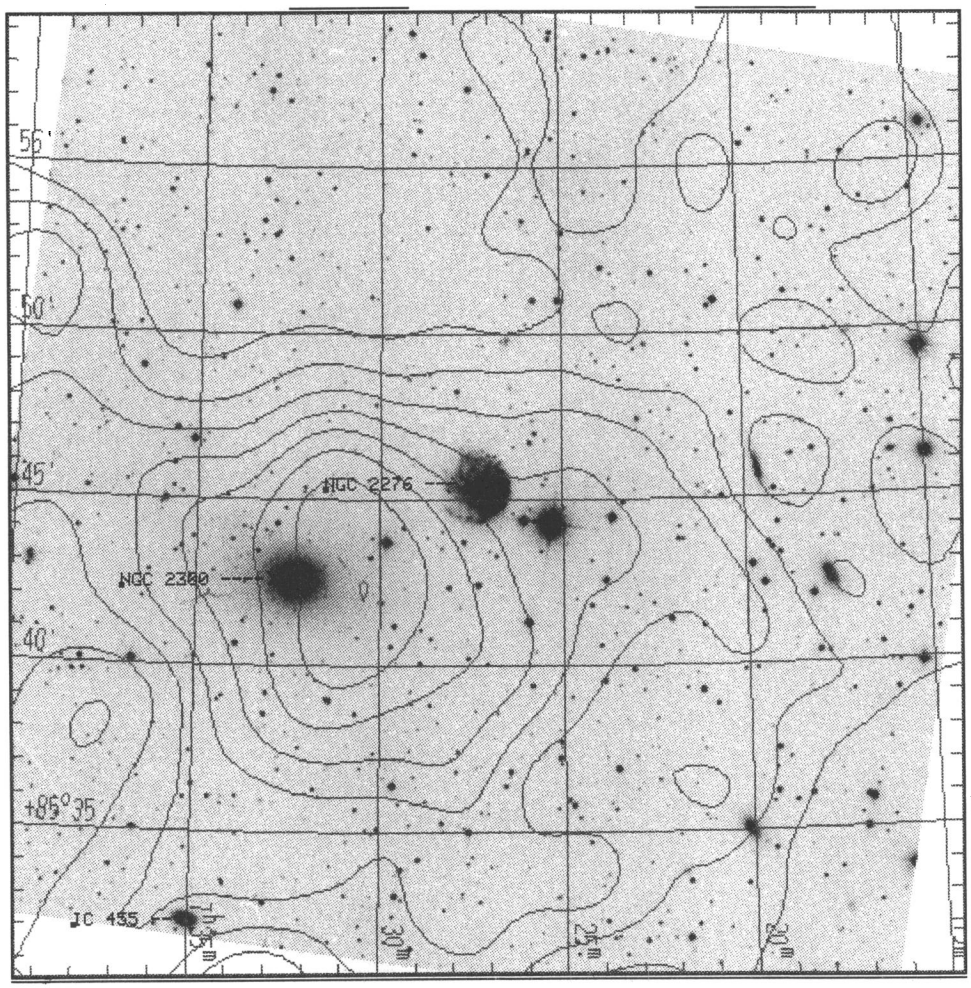

FIG. 2.—Smoothed X-ray data (σ = 1.5) with all point sources removed as described in the text is overlaying the same optical image as Fig. 1. The contour levels are (2.62, 3.13, 3.74, 4.46, 5.33, 6.36, 7.59) × 10^{-4} counts s^{-1} $arcmin^{-2}$.

summed data. Instead, we fitted the three *ROSAT* spectra simultaneously using XSPEC. Since each spectrum is from the same physical position on the sky we require that the temperature and abundance of all three fits be the same. We also fixed the value of the Galactic absorption (N_H) to be 4.25×10^{20} cm^{-2} (Stark et al. 1992) found at the position of the X-ray peak. The data were fitted in the energy range from 0.4 to 2.0 keV with both the temperature and abundance as free parameters. The best-fit spectrum is shown in Figure 4 and has a temperature of $0.97^{+0.11}_{-0.08}$ keV with an abundance of $0.06^{+0.05}_{-0.02}$ solar. The confidence contours for the temperature and abundance are shown in Figure 5. The flux from the source is 3.14×10^{-12} erg s^{-1} cm^{-2} in the 0.4–2.0 keV band, and this corresponds to a luminosity of 7.89×10^{41} ergs s^{-1}. The bolometric flux is 4.46×10^{-12} erg s^{-1} cm^{-2}, and the bolometric luminosity is 1.12×10^{42} ergs s^{-1}. Fixing the abundance to the best-fit value and allowing the N_h to vary changes the best-fit temperature slightly to $0.92^{+0.10}_{-0.09}$ keV, and the fitted Galactic column is $5.08^{+4.34}_{-1.32} \times 10^{20}$ cm^{-2}.

With the additional observations dividing the data into radial bins and fitting the spectrum from the three annuli is now possible. We extract data for radii of 0′ to 8′ (0–0.11 kpc), from 8′ to 16′ (0.11–0.24 kpc), and from 16′ to 25′ (0.24–0.33 kpc). We fitted the data from these regions in the same manner as the entire spectrum and the results are presented in Table 2 and Figure 6. As can be seen, neither the temperature or abundance of the gas appear to have a significant radial gradient.

5. MASS DETERMINATIONS

Until X-ray gas was detected in groups with sufficient photon statistics to determine both the radial extent and the spectral properties of the gas, determining the mass for individual poor groups was very uncertain. The small number of galaxies comprising the group renders the optical methods of determining the group velocity dispersion and true extent of the group subject to large errors. However, the presence of large amounts of dark matter in these groups can be inferred statistically by investigating the velocity dispersions of many groups (see, e.g., Gott & Turner 1977; Nolthenius 1993). This method shows that groups, if bound, have large amounts of dark matter. The presence of hot gas trapped in the potential well of the NGC 2300 group provides a measure of the mass of an individual group and is a powerful argument for the presence of large amounts of dark matter in this group.

The use of X-ray measurements of hot gas to determine the total mass of a system depends on several assumptions, the prime one being that the gas is in equilibrium with the underlying potential. The advantage of using the gas is that it relaxes on its sound crossing time that is much less than the time for the galaxies to relax. The binding mass can be

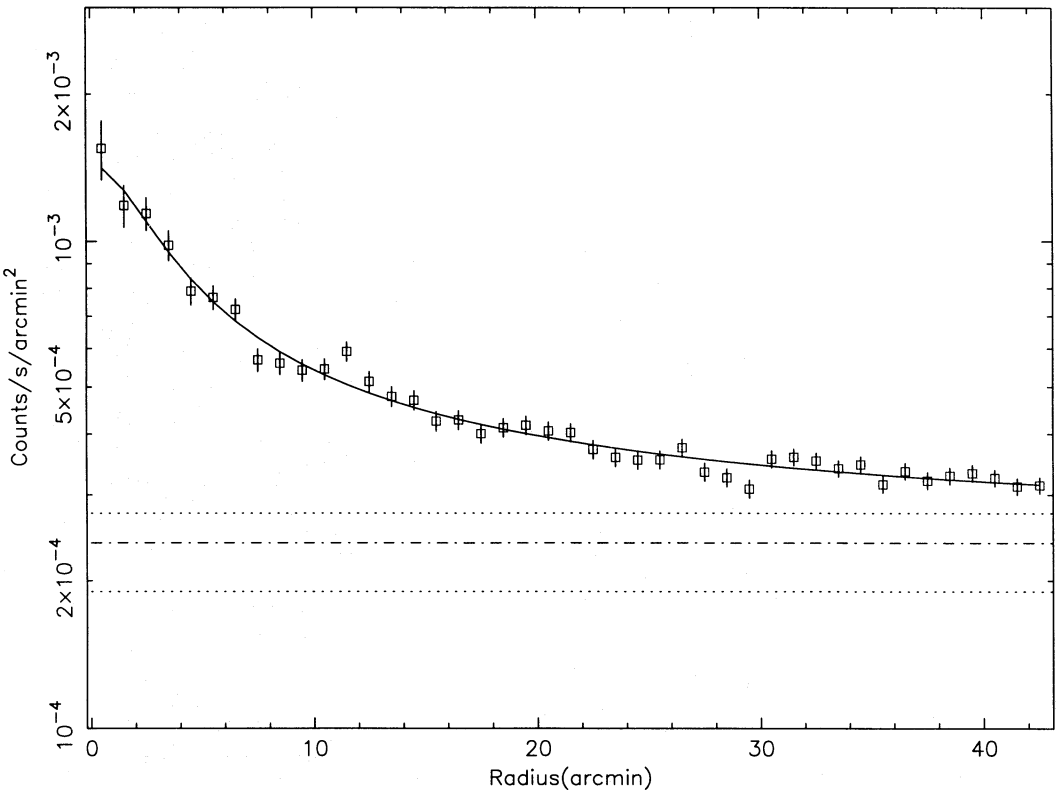

FIG. 3*a*

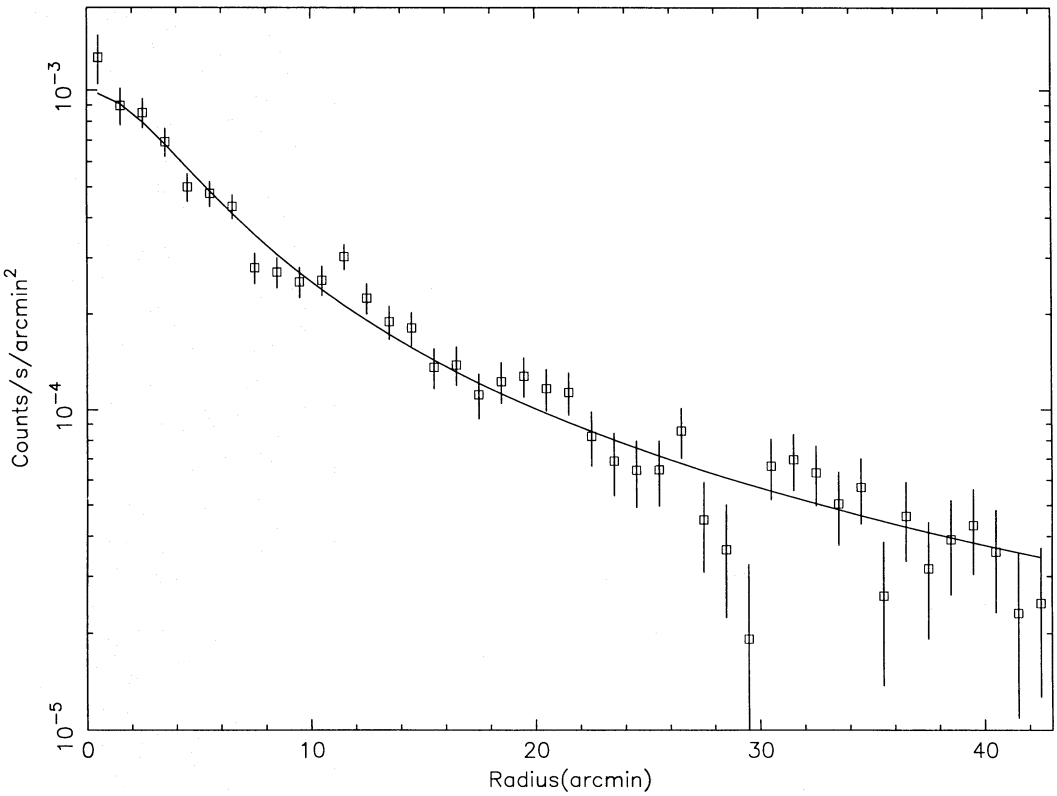

FIG. 3*b*

FIG. 3.—(*a*) Surface brightness profile of the diffuse gas before the best-fit background has been removed. The dashed line is the background fit to the data without the model of the group gas. The dotted lines above and below the solid line are the 90% confidence upper limit and 90% confidence lower limit to the background. The solid line shows the King model plus a constant background fit to the data. (*b*) Surface brightness profile of the diffuse gas after the best-fit background has been removed. The solid line is the King model fit to the data.

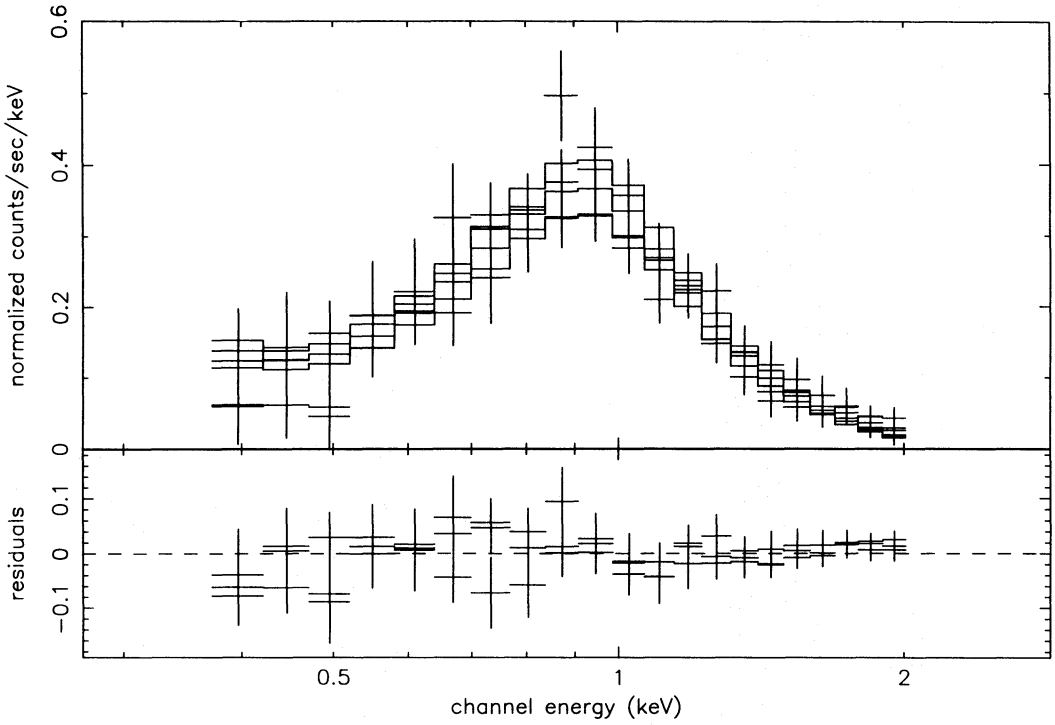

FIG. 4.—X-ray spectrum from the group is shown in the upper panel along with the best-fit Raymond-Smith plasma model (*solid line*). The lower panel shows the residuals to the best fit.

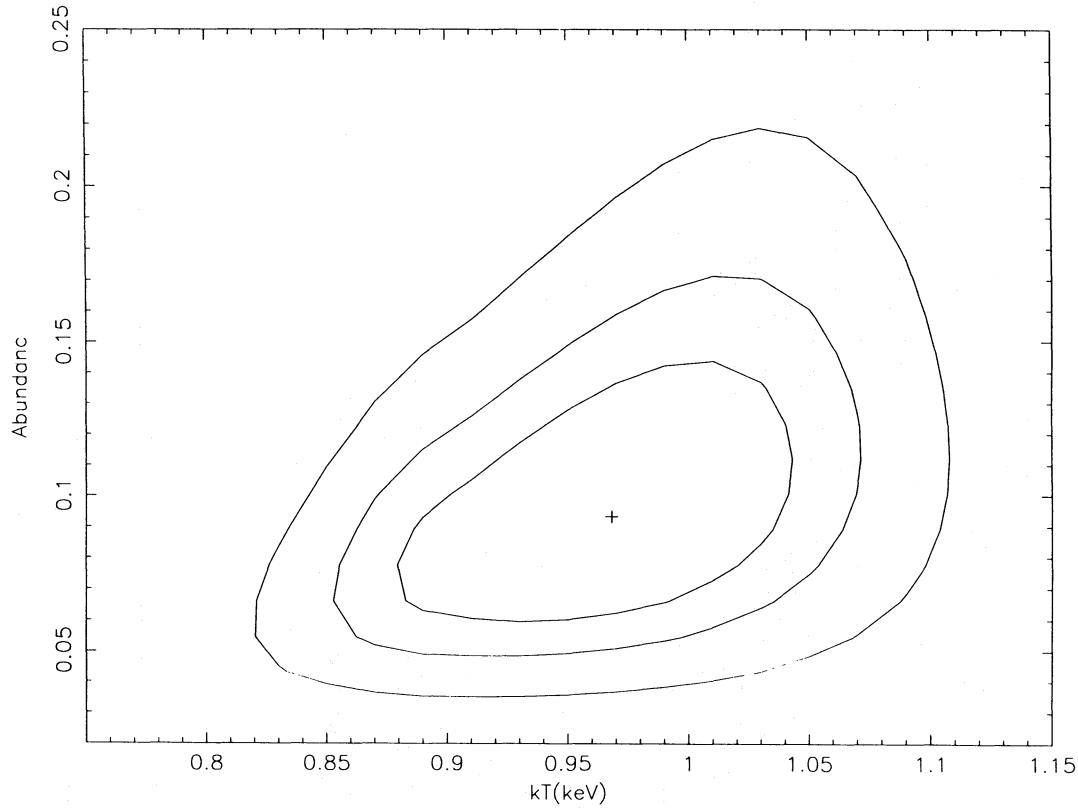

FIG. 5.—90% confidence parameters for the temperature and abundance are shown here

TABLE 2

SPECTRAL PARAMETERS FOR THE NGC 2300 GROUP

Counts	kT (keV)	Abundance	N_H (cm^{-2})	χ^2/d.o.f.	Radii
6147.....	$0.97^{+0.08}_{-0.10}$	0.05–0.12	5.08×10^{20}	37/57	0′–25′
1524.....	$0.97^{+0.12}_{-0.14}$	0.07–0.32	5.08×10^{20}	21/57	0–8
2612.....	$0.98^{+0.11}_{-0.12}$	0.04–0.18	5.08×10^{20}	26/57	8–16
2011.....	$0.86^{+0.21}_{-0.13}$	0.03–0.19	5.08×10^{20}	37/57	16–25

TABLE 3

FITTED PARAMETERS FOR THE NGC 2300 GROUP

Background	Counts (s^{-1} arcmin^{-2})	R_{core}	β	S_0 (counts s^{-1} arcmin^{-2})
"Best"	2.39×10^{-4}	4.′28 (56.5 kpc)	0.41	9.87×10^{-4}
"Max".....	2.75×10^{-4}	8.′05 (107.0 kpc)	0.60	7.65×10^{-4}
"Min"	1.90×10^{-4}	2.′57 (33.9 kpc)	0.33	11.93×10^{-4}

derived using the equation of hydrostatic equilibrium:

$$M(<r) = -\frac{kTr}{G\mu m_p}\left(\frac{d\ln n}{d\ln r} + \frac{d\ln T}{d\ln r}\right), \quad (2)$$

which, for a polytropic gas, can be written as

$$M(r) = 2\gamma\delta\,\frac{kTr}{G\mu m_p}\,\frac{x^3}{(1+x^2)^{1+\delta(\gamma-1)}} \quad (3)$$

(Cowie, Henriksen, & Mushotzky 1987), where m_p is the mass of the proton, μ is the mean molecular weight, and $x = r/R_{core}$. For an isothermal distribution $\gamma = 1$ and $\delta \approx 1.5\beta/[1 - 0.2(\gamma - 1)]$ or $\delta = 1.5\beta$ for an isothermal distribution, which is a good description of our data. Using the value of β and the core radius from the surface brightness fitting, we find the binding mass to be $1.47^{+0.19}_{-0.20} \times 10^{13}\ M_\odot$ and the gas mass to be $1.25^{+0.13}_{-0.12} \times 10^{12}\ M_\odot$ within a radius of 0.33 Mpc. This constrains the gas fraction to be between 7% and 14% . Using the mass of the galaxies as determined by Mulchaey et al. (1993) of $\sim 6 \times 10^{11}\ M_\odot$ we find the baryonic fraction to be between 10%–16%. If a temperature gradient does exist in the gas, then the range for the allowed baryonic fraction will increase.

To determine how the background affects the fitted and derived group parameters we have produced surface brightness profiles using the best-fit background, from the above analysis, but also the upper and lower limits of the background allowed at the 90% level. Table 3 lists the fitted parameters for the group using the best-fit background, the maximum background (90% confidence upper limit), and the minimum background (90% confidence lower limit). The third column of the table lists the background value used, the second column gives the derived core radius in arcmin and kpc, the next column lists β, and the last column contains the central surface brightness for the diffuse gas. The values given in Table 3 are used to determine the central electron density, gas mass, and total gravitating mass. Table 4 lists these values in columns (2), (3), and (4) along with the gas fraction and baryonic fraction on columns (5) and (6). The last line of Table 4 lists the values we determined for the initial analysis of the NGC 2300 group data (Mulchaey et al. 1993).

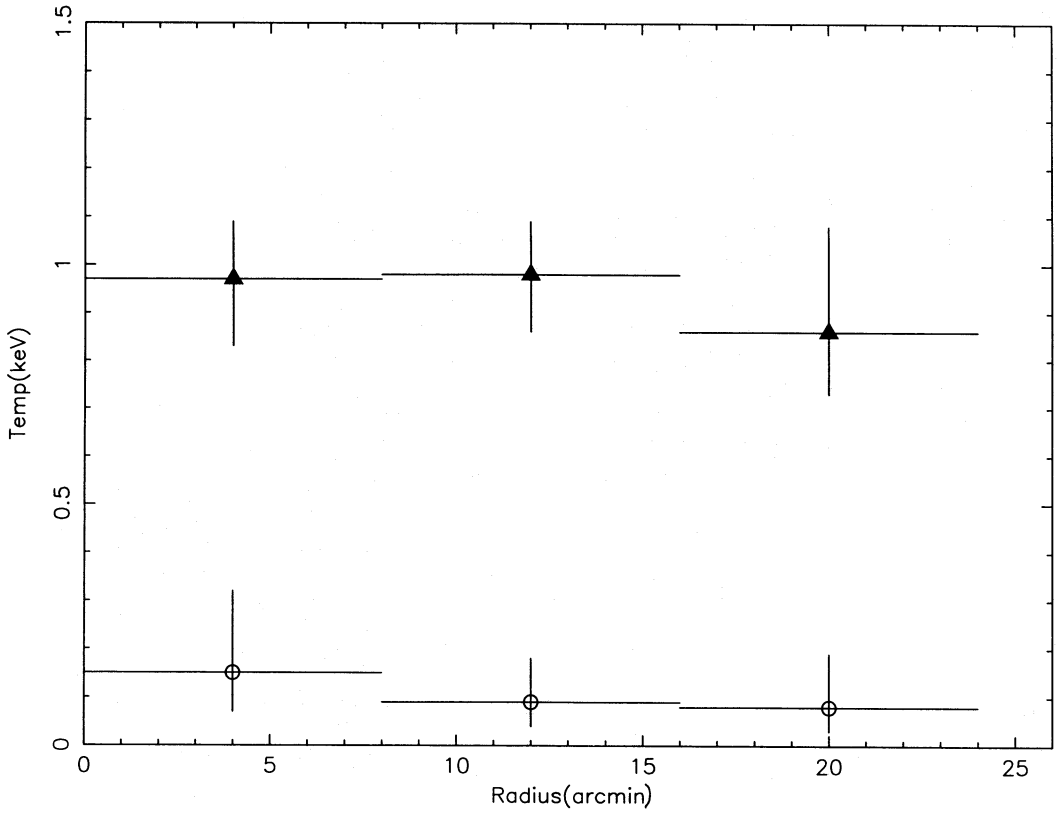

FIG. 6.—Radial temperature profile for the group gas is shown using the solid triangles, and the radial variation of the fitted abundance is shown using the open circles. The vertical error bars are the 90% confidence range for one interesting parameter.

TABLE 4

DERIVED PARAMETERS FOR THE NGC 2300 GROUP

Background (1)	n_0 ($\times 10^{-3}$ cm^{-3}) (2)	M_{gas} ($M_\odot$) (3)	M_{total} ($M_\odot$) (4)	f_{gas} (5)	$f_{baryons}$ (6)
"Best"	3.11	1.25×10^{12}	1.47×10^{13}	8.5%	12.6%
"Max"	0.42	1.84×10^{12}	2.00×10^{13}	4.8%	7.9%
"Min"	4.65	3.02×10^{11}	1.20×10^{13}	13.2%	18.3%
"Old"	...	$<5.11 \times 10^{11}$	2.0×10^{13}	7.9%	<20%

6. ABUNDANCE OF THE DIFFUSE GAS

The initial observation of the NGC 2300 group has been reanalyzed by Pildis et al. (1995) and by David et al. (1995). Both of these groups confirm the principal conclusion of our initial analysis: that this group has cool X-ray emitting gas associated with it. All three analyses of the *ROSAT* data have found the temperature of the gas is around 1 keV, and this is confirmed by the analysis of the *ASCA* data (Tawara et al. 1995). The radial extent of the detected gas varies between 0.21 Mpc (Pildis et al. 1995) to 0.33 Mpc (Mulchaey et al. 1993; this work). This variation in radius is most likely due to the various backgrounds adopted. David et al. quote the radius of the group at 20% of the background they used ($R_{20} = 0.20$ Mpc).

We note that the baryonic fraction we derive from our new analysis is consistent with the recent estimates made for this group by Pildis et al. (1995) and David et al. (1995), but considerably higher than the best-fit value of 6% found in our original paper (see note added in proof in Mulchaey et al. 1993). This difference can be attributed to differences in the gas density profile used in the baryonic fraction calculation. In our initial paper $\beta = 0.66$ was *assumed*. (We mistakenly sent Henriksen & Mamon 1994 $\beta_{spec} = 0.85$; however, the background they used was higher than the one used in the original analysis.) Our present analysis, as well as the analysis of Pildis et al. (1995) and David et al. (1995), suggests the true radial profile of the gas is significantly flatter.

Thus, the true gas mass and overall baryonic fraction was underestimated in Mulchaey et al. (1993). Our present estimate for the baryonic fraction in the NGC 2300 group (i.e., 10%–16%) is consistent with the range found for other small groups with diffuse gas (Pildis et al. 1995; Mulchaey et al. 1996). However, the derived baryonic fractions are still rather uncertain and a sensitive function of the background level adopted (see Henriksen & Mamon 1994).

The relatively coarse spectral resolution of the *ROSAT* PSPC, which blends individual lines, makes the determination of the metal abundance difficult. For the PSPC spectra a model with the appropriate metal abundance is convolved with the instrumental response and then compared with the data to determine the goodness of fit. The Fe L complex in low-temperature plasmas provides a sensitive measure of the amount of iron in the plasma. Modeling PSPC spectra of a Raymond-Smith plasma with $kT = 1$ keV and various abundances show that this detector is quite sensitive to the presence of iron. Our best-fit abundance for the group gas of 0.06 solar (Mulchaey et al. 1993) is confirmed by the additional PSPC data we have acquired. The NGC 2300 group has also been observed by *ASCA*. The *ASCA* SIS detectors have much better spectral resolution than the PSPC, and individual line complexes can be easily separated from the continuum emission. This makes the determination of abundances much less model dependent than for the PSPC data. In the analysis of the *ASCA* data for this group Tawara et al. (1995) show that the abundance is between 0.04 and 0.13 solar, in excellent agreement with the PSPC values. For completeness, Table 5 compares the parameters we have determined for this group to those others have published.

7. DISCUSSION

7.1. *Group Mass*

The ability of the hot X-ray gas to relax on short timescales, much shorter than the galaxies, makes this gas a much more reliable tracer of the potential of a system and thus provides a much more robust estimate of the mass. The presence of hot gas in poor groups allows the mass of these systems to be determined using the same techniques used to determine the mass of much richer clusters. For poor groups this is the *only* method to reliably measure the mass for an individual group, given the handful of galaxies in these systems.

The accuracy of the mass determination from the X-ray data depends upon the accuracy of the assumption that the gas is in hydrostatic equilibrium with the group potential. The X-ray contours in the central 8′ are elongated in a north-south direction. If the region within 2′ of the giant

TABLE 5

PARAMETERS FOR THE NGC 2300 GROUP FROM THE LITERATURE

Counts	kT (keV)	A Solar	Extent (Mpc)	M_{gas} ($\times 10^{11} M_\odot$)	M_{total} ($\times 10^{13} M_\odot$)	M_{Bary}/M_{total}	Reference
2047	0.72–1.01	0.01–0.18	0.3	<5.0	1.5–2.4	<0.2	1
838 ± 131	0.73–1.13	...	0.21	0.52	0.70	0.14	2
...	0.73–0.96	...	0.20[a]	...	0.76	0.10–0.13	3
1203	0.76–1.03	0.04–0.13	>0.33[5]	...	...	...	4
6147	0.87–1.05	0.05–0.12	0.33	11.3–13.8	1.27–1.66	0.104–0.156	6

[a] Measured at 20% of the background.

REFERENCES.—(1) Mulchaey et al. 1993; (2) Pildis et al. 1995; (3) David et al. 1995; (4) Tawara et al. 1995; (5) Tawara 1994; (6) this work.

elliptical is ignored, then the contours are fairly round, indicating that at least the central part of the group gas is in equilibrium with the underlying potential. At radial distances greater than about 8′ the low counting rate from the diffuse gas makes following individual contour lines difficult. However, dividing the data into four quadrants and examining the radial profile indicates that there are no large-scale variations in the X-ray emission in the outer regions of the group.

Arguments by Ashman (1992) indicate that for a system to be in virial equilibrium at the current redshift, it must have a density of at least $5.8 \times 10^{13}\ M_{\odot}\ \mathrm{Mpc}^{-3}$. The NGC 2300 group has a mass of $1.47 \times 10^{13}\ M_{\odot}$ within a projected radius of 0.33 Mpc. Assuming spherical symmetry, the density of this system is $9.8 \times 10^{13}\ M_{\odot}\ \mathrm{Mpc}^{-3}$, indicating that this system has sufficient density such that it may be virialized. The temperature of the X-ray gas can be used as a measure of the depth of the potential well in which it resides. If we assume that the density given by Ashman (1992) is the minimum density for a structure to be virialized, and that these structures all formed at a similar epoch, then we can relate the X-ray temperature to the radius of virilization (Bird 1995) by

$$r_{\mathrm{vir}}^2 \propto T_{\mathrm{X}}\ , \tag{4}$$

where T_{X} is the measured X-ray temperature and r_{vir}^2 is the radius to which the structure is virialized at the present epoch. We use a well-studied cluster, Coma, to define the fiducial values. Coma has a global X-ray temperature of $8.4^{+1.1}_{-0.9}$ keV (Watt et al. 1992), and we assume that it is in virial equilibrium to approximately its Abell radius ($3\ h_{50}^{-1}$ Mpc; Bird 1995; The & White 1986). Using these values we find that the NGC 2300 group's virial radius is ~ 1 Mpc. While using such a massive system as Coma to extrapolate to poor groups is probably very uncertain, no poor systems have been studied sufficiently to determine a virial radius. In any case, these arguments indicate that the group gas may be in equilibrium with the group potential, and thus our assumption of hydrostatic equilibrium should yield fairly accurate parameters for the NGC 2300 group. Confirmation comes from recent numerical work (Diaferio, Geller, & Fabricant 1996), which indicates that within 200 kpc the X-ray analysis tends to underestimate the true mass by about 20%.

7.2. *Enrichment of the Diffuse Gas*

The enrichment process for clusters is still a matter of some debate. Heavy elements such as iron are only produced in stellar interiors, while cluster gas is thought to be primarily from the infall of metal-free primordial gas. X-ray observations show that the hot gas, in the interior regions of clusters, is enriched with heavy elements that are from stellar processes. The problem is how enriched material processed through stars is transported from the galaxies to the cluster gas. Two processes that may be acting in clusters are galactic winds and stripping of the galactic interstellar medium. Clusters of galaxies are relatively complex systems where both processes can remove gas from the galaxies. Poor groups are much simpler systems with few galaxies, and in many cases the density of the hot gas is not large enough for stripping to be an important process.

In the stripping model supernovae enrich the gas in the galaxy. This enriched gas is then stripped from the galaxy by ram pressure as the galaxy moves though the cluster gas. So over time the metals produced by galactic supernovae are deposited in the cluster gas. This process works well for rich clusters where the intracluster gas is relatively dense. However, for less dense environments, intermediate and poor clusters, stripping should be less efficient since the gas density in these systems is less than those in rich clusters. For very diffuse gas seen in groups the stripping of the gas from normal galaxies should not happen. Since the low density of the group gas in the NGC 2300 group makes stripping of the gas from galaxies improbable, we will not consider the stripping scenario further.

Observationally, the hot gas confined in the potential well of this group remains among the lowest abundance extragalactic gas detected in the X-rays. This is in contrast to what is expected from the X-ray data for clusters. Hatsukade (1989) showed that the abundance of iron *increases* in poorer clusters. If this relationship is extrapolated to groups ($kT = 1$), then the iron abundance is predicted to be greater than about 0.6 solar. This is a factor of 10 greater than is seen in the NGC 2300 group. However, *ROSAT* observations of groups seem to show a wide range of abundances (Mulchaey et al. 1996; Davis et al. 1995; David et al. 1994; Ponman & Bertram 1993). In principle, the wide variation of abundance in such relatively simple systems provides a unique test for the enrichment process for the diffuse hot gas.

The alternate model to the stripping model is the wind model. In this model the supernova that enrich the gas also heats the gas. In the early phases of the formation of an elliptical galaxy the numerous supernovae can heat the gas enough so that the galaxy can no longer retain the gas and a wind forms. David, Forman, & Jones (1991) have modeled this process and find that all their models for elliptical galaxies form winds and all but the low-luminosity ellipticals maintain these winds until the present epoch. This model reproduces the increasing abundance with decreasing richness well and thus it seems natural to test this model with the most extreme systems—poor groups.

The galaxy mass in this group is dominated by NGC 2300, an elliptical with $L_{\mathrm{B}} = 5.4 \times 10^{10}\ L_{\odot}$. To determine the effects of winds from the elliptical we will use the models presented by David et al. (1991). We use their model results for an elliptical galaxy with $L_{\mathrm{B}} = 10^{10}\ L_{\odot}$ and supernova rates of 0.25, 0.10, and 1.0 per year and the slope of the initial mass function for a Salpeter mass law is 1.5. For each of the various supernova rates the total energy output in the wind is $\sim 4.2 \times 10^{59}$ ergs. This is only $\sim 4\%$ of the total energy in the group gas and so is not a significant energy input. The mass expelled from the galaxy is $\sim 1.2 \times 10^{10}\ M_{\odot}$, which contains $5.3 \times 10^{7}\ M_{\odot}$ of iron. The fraction of the gas from the galaxy compared to that in the group is only 5.1×10^{-3}, while the fraction of iron that should be injected into the gas is 2.3×10^{-5}. That is about half the solar value of 4.68×10^{-5} and predicts that the observed abundance would be ~ 0.5 solar. However, the measured abundance of iron is only ~ 0.06 solar, much less than what is predicted by the wind model. If the wind model is correct then to dilute the iron so that the observed abundance is reproduced the ejected iron must have been mixed with $\sim 2 \times 10^{13}\ M_{\odot}$ of primordial gas. To have such a large reservoir of hot gas we must extend our best-fit model to ~ 1.5 Mpc, much further than observed. A further constrain on the wind model comes from the uniform distribution of temperature and metallicity. A wind would preferentially

deposit metals and energy in the inner part of the group. The lack of an observable temperature or metallicity gradient indicated that either the gas has been well mixed after the wind phase of the elliptical was finished or, as discussed below, the elliptical fell into the group recently.

One method of solving the discrepancy between the predicted and observed gas abundance is to have the group gas and the galaxy separate during the early evolution of the elliptical. So either the elliptical or the gas has only recently fallen into the group. Alternately, the predictions of the David et al. model may not be correct. Assuming the model predictions are correct, we can assess the chances of either of above two cases occurring. If NGC 2300 has only recently fallen into the group, it is difficult to understand why it lies so close to the peak of the X-ray emission. The crossing time for a galaxy in the group is about $\sim 6 \times 10^9$ yr. Simulations show that several crossing times are required for a galaxy to settle into the center of the group. This would make it unlikely that the elliptical would be seen in the group center. Also, for most groups with diffuse X-ray emission the elliptical appears to lie close or at the center of the X-ray emission (Mulchaey et al. 1996). So unless the NGC 2300 group is quite different, it seems unlikely that NGC 2300 is just now falling into the group.

For the case with the gas falling in recently the gas can relax more quickly than the galaxies. An estimate of the time for the gas to relax is given by the sound crossing time:

$$t_s = 6.6 \times 10^8 \left(\frac{T_{\rm gas}}{10^8 \text{ K}} \right)^{-0.5} \left(\frac{D}{\text{Mpc}} \right) \text{yr} , \qquad (5)$$

where T_g is the gas temperature and D is the diameter of the group (Sarazin 1986) and is $\sim 7 \times 10^8$ yr for the group gas. So the gas could have fallen into the group and reached equilibrium after NGC 2300 had expelled, and the group lost, most of the metal-rich gas. However, the problem remains of how the primordial gas, with low metal abundance, did not trap the wind from the elliptical and return it to the group. One possible explanation is that the primordial gas fell into the group as clouds. This would allow the wind to escape and the clouds would not trap a significant fraction of the metal-rich gas and return it to the group. This scenario is also discussed in Renzini et al. (1993).

Diaferio, Geller, & Ramella (1994) have recently proposed a model for the evolution of compact groups in which groups may be continuously evolving. In their simulations they show that compact groups form continuously, so as the inner members of the group merge into a central object galaxies from further out replace the merged objects. The simulations are specifically for rich groups. If this scenario applies to poor groups as well (Diaferio et al. 1996), then the low elemental abundance in the group gas may be explained by simply having a much less luminous elliptical in the past. In fact if NGC 2300 was an order of magnitude less luminous in the past, then the models of David et al. (1991) predict approximately the correct mass of iron.

Evidence for NGC 2300 undergoing a merger event is presented in Forbes & Thomson (1992), who show that NGC 2300 has shells and a tidal extension. They attribute the tidal extension to an interaction with NGC 2276 (Arp 114), but shells are thought to form during a merger event (see, e.g., Quinn 1984; Duprez & Combes 1986; Hernquist & Quinn 1988, 1989). Such shells are the remnants of a companion galaxy that has been disrupted by the more massive elliptical during a merger. These shells provide strong evidence that NGC 2300 has undergone at least one merger in the recent past.

Finally the low abundance of the diffuse gas in the NGC 2300 group can also be achieved if the metal-rich gas from the elliptical is diluted in a large amount of primordial gas. However, such a large amount of gas is not seen in the X-ray data or in the available H I data (Huchtmeier 1994). Mulchaey et al. (1996) postulate that cool gas ($kT < 0.3$ keV) may be present in many groups. Gas with temperatures at or below about 0.3 keV would be difficult to detect with the *ROSAT* PSPC because of the Galactic X-ray background and for gas at lower temperatures the sensitivity of the PSPC to cool gas drops dramatically. Thus, if the NGC 2300 group is surrounded by a reservoir of cool gas it would be difficult to detect. If the NGC 2300 group is surrounded by gas with a temperature below 0.3 keV, we would expect that the wind energy from NGC 2300 would heat at least part of this cool gas. We observe $1.25 \times 10^{12}\ M_\odot$ of gas and the energy input required to heat this amount of gas to the observed temperature is $\sim 4 \times 10^{60}$ ergs. The wind energy predicted by David et al. (1991) for a $10^{10}\ L_\odot$ elliptical is $\sim 4 \times 10^{59}$ ergs, an order of magnitude below what is required to heat the gas from 0.3 to 1 keV. While this factor may possibly be within the uncertainty in the model, this does not solve the problem of the low abundance of the diffuse gas, since the wind should enrich the gas as well as heat it. Thus, there must be a source of low-abundance gas that can dilute the metal-rich gas from the elliptical and be heated by another means. One method of achieving this is to have a reservoir of cool gas that can fall into the group and be mixed with the metal-rich gas from the elliptical. Then the temperature of the X-ray emitting gas would reflect the depth of the potential well of the group.

We note that the models used here for the evolution of ellipticals are rather simple. David et al. (1991) use IMFs with slopes between 1.0 and 2.0 to produce the supernovae that drive the stellar winds and enrich the gas. In fact, the low abundance of hot gas in ellipticals seems to rule out such models with the Tammann (1994) Type I supernova rate (Lowenstein et al. 1995). Models of the evolution of elliptical galaxies that fit the clusters abundances also require flat or bimodal IMF (Lowenstein & Mushotzky 1996). This might solve the problem of the low metallicity we observe in the group gas but is not consistent with the metallicity measured in cluster gas. So either the models for elliptical evolution used by David et al. are too simple, or large amounts of primordial gas must dilute the metal-rich gas.

The failure of any one mechanism to explain both the temperature and low abundance of the diffuse gas indicates that even for simple systems, like poor groups, the evolution of the intergroup medium can be complex and is not dominated by any single process. The evidence for past merger events in NGC 2300 complicates any scenario where winds from the elliptical are used to enrich and heat the diffuse gas. The study of more groups should help determine if the NGC 2300 group is unusual because of its past merger activity or typical of poor groups.

8. CONCLUSIONS

We have verified the presence of diffuse, low-abundance, X-ray emitting gas in the NGC 2300 group. The best-fit

temperature of 0.97 keV is in good agreement with the original data for this group. The derived abundance is in excellent agreement with that determined from the original analysis (Mulchaey et al. 1993) and from *ASCA* SIS observations (Tawara et al. 1995).

Using our best-fit background the total gravitating mass of this group is $1.47 \times 10^{13}\ M_{\odot}$ within 0.33 Mpc, and the gas mass is $1.25^{+0.13}_{-0.12} \times 10^{12}\ M_{\odot}$ within the same radius. This constrains the gas fraction to be between 7% and 14%. Using the mass of the galaxies as determined by Mulchaey et al. (1993) of $\sim 6 \times 10^{11}\ M_{\odot}$, we find the baryonic fraction to be between 10%–16%, well within the error range of the original analysis, but above the best-fit value of 6% we derived by fixing the value of β at 0.66.

We have also shown that fitted parameters of this group are quite sensitive to the background used. Using the maximum and minimum allowed values of the background, we find that the gas mass can vary between $3.0 \times 10^{11}\ M_{\odot}$ and $1.8 \times 10^{12}\ M_{\odot}$. Using these values the baryonic fraction can range from a low of 8% to a high of 18%.

A comparison of these observations with wind models for the enrichment of cluster gas has also been presented. Using the models for elliptical evolution from David et al. (1991), we show that straightforward methods of enriching the group gas over produces the amount of iron in the gas by a factor of 10. However, if NGC 2300 was much less luminous in the past then their models can produce roughly the correct amount of gas. An alternate scenario is that most of the gas around the group is cool, less than 0.3 keV, and is difficult to observe with the PSPC. Then the enriched gas from the elliptical can be mixed with a much larger mass of gas to reproduce the low abundance. This solves the problem of the observed abundance, but then it is unclear how the gas in the center is heated to the observed temperature. To distinguish between these scenarios more detailed modeling of the evolution of ellipticals, poor groups, and the interaction of winds with diffuse gas must be done.

We would like to thank Ray White and Mark Henriksen for useful discussions. This research made use of the HEASARC, NED, and SkyView databases and was supported in part by NASA grant NAG 5-2455. We would also like to thank the referee, Trevor Ponman, for his comments, which helped to improve the paper.

REFERENCES

Ashman, K. M. 1992, PASP, 104, 1109
Bird, C. M. 1995, ApJ, 445, L81
Böhringer, H. 1994, in Clusters of Galaxies, the 14th Moriond Astrophysics Meeting, ed. F. Darret, A. Mazure, & J. Tran Thanh Van (Gif-sur-Yvette: Editions Frontiéres), 139
Cavaliere, A., & Fusco-Femiano, X. 1976, A&A, 49, 137
Cowie, L. L., Henriksen, M., & Mushotzky, R. F. 1987, ApJ, 317, 593
David, L. P., Forman, W., & Jones, C. 1991, ApJ, 380, 39
———. 1995, preprint
David, L. P., Jones, C., Forman, W., & Daines, S. 1994, ApJ, 428, 554
Davis, D. S., Mushotzky, R. F., Mulchaey, J. S., Worrall, D., Birkinshaw, M., & Burstein, D. 1995, ApJ, 444, 582
Diaferio, A., Geller, M. J., & Fabricant, D. 1996, in preparation
Diaferio, A., Geller, M. J., & Ramella, M. 1994, AJ, 107, 868
Duprez, C., & Combes, F. 1986, A&A, 166, 53
Forbes, D. A., & Thomson, R. C. 1992, MNRAS, 254, 723
Gott, R., III, & Turner, E. L. 1977, ApJ, 213, 309
Hatsukade, I. 1989, Ph.D. thesis, Osaka Univ.
Henriksen, M. J., & Mamon, G. A. 1994, ApJ, 421, L63
Hernquist, L., & Quinn, P. J. 1988, ApJ, 331, 682
———. 1989, ApJ, 342, 1
Huchtmeier, W. 1994, A&A, 286, 389
Lowenstein, M., & Mushotzky, R. F. 1996, ApJ, submitted
Lowenstein, M., Mushotzky, R. F., Tamura, T., Ikebe, Y., Makishima, K., Matsushita, K., Awaki, H., & Serlemitsos, P. J. 1995, ApJ, 436, L75
Mulchaey, J. S., Davis, D. S., Mushotzky, R. F., & Burstein, D. 1993, ApJ, 404, L9
———. 1996, ApJ, 456, 80
Nolthenius, R. A. 1993, ApJS, 85, 1
Pildis, R. A., Bregman, J. N., & Evrard, A. E. 1995, ApJ, 443, 514
Quinn, P. J. 1984, ApJ, 279, 596
Ponman, T. J., & Bertram, D. 1993, Nature, 363, 51
Renzini, A., Ciotti, L., D'Ercole, A., & Pellegrini, S. 1993, ApJ, 419, 52
Saracco, P., & Ciliegi, P. 1995, A&A, in press
Sarazin, C. L. 1986, Rev. Mod. Phys., 58, 1
Snowden, S. L., McCammon, D., Burrows, D. N., & Mendenhall, J. A. 1994, ApJ, 424, 714
Stark, A. A., Gammie, C. F., Wilson, R. W., Bally, J., Linke, R. A., Heiles, C., & Hurwitz, M. 1992, ApJS, 79, 77
Sulentic, J. W., Pietsch, W., & Arp, H. 1995, A&A, 298, 420
Tammann, G. A. 1974, in Supernovae and Supernovae Remnants, ed. C. B. Cosmovici (Dordrecht: Reidel), 155
Tawara, Y., Sakima, Y., Yamashita, K., & Mushotzky, R. 1995, in Proc. 5th Annual October Astrophysics Conf. in Maryland, Dark Matter, ed. S. Holt & C. L. Bennett (New York: AIP), 268
The, L. S., & White, S. D. M. 1986, AJ, 92, 1248
Thiering I., & Dahlem, M. 1996, in preparation
Watt, M. P., Ponman, T. J., Bertram, D., Eyles, C. J., Skinner, G. K., & Willmore, A. P. 1992, MNRAS, 258, 738